Synthesis and Characterization of $Ta_2Ni_3Se_8$

Yongkwan Dong, Junghwan Do, Hoseop Yun*, Youngju Lee†, Heekyoon Shin†, and Kwangkyoung Liou‡

Department of Chemistry, †Department of Physics, Ajou University, Suwon 442-749, Korea
‡Departmemt of Chemistry, Sun Moon University, Asan 337-840, Korea
Received June 21, 1995

A new ternary transition-metal selenide, $Ta_2Ni_3Se_8$ has been synthesized from a eutectic halide flux. The structure of this phase has been characterized by single crystal X-ray diffraction techniques. The compound crystallizes in the orthorhombic system (D_{2h}^9-*Pbam*, $a=14.788(4)$ Å, $b=10.467(3)$ Å, $c=3.4563(8)$ Å) with two formula units in the unit cell. This compound adopts the $Nb_2Pd_3Se_8$ structure type. Hence, there are two chains of edge-sharing selenium trigonal prisms centered by tantalum atoms and these chains are interconnected through two kinds of nickel atoms. Nickel occupies both square planar and square pyramidal sites as does palladium in $Nb_2Pd_3Se_8$. Electrical conductivity measurements indicate that this material is semiconducting.

Introduction

Considerable efforts in modern solid state materials research have been focused on transition metal chalcogenides with anisotropic structures. This research has been motivated by the search for new materials with interesting properties such as superconductivity,[1] application as battery materials,[2] charge density waves(CDW),[3] ionic conductivity,[4] and magnetic properties.[5] Especially, $Nb_2Pd_3Se_8$[6,7] and its isostructures, $Ta_2Pd_3Se_8$,[7,8] $Ta_2Ni_3S_8$, and $Ta_2Pt_3Se_8$,[7,9] have been synthesized through the direct combination of constituent elements at an elevated temperature and investigated intensively. However, efforts to extend this system to other substitutional phases via traditional solid state synthetic route have not been successful yet. In an attempt to prepare quaternary metal chalcogenides by the use of the reactive eutectic halide flux methods, $Ta_2Ni_3Se_8$ was obtained instead. In the report, the synthesis and characterization of a new ternary chalcogenide, $Ta_2Ni_3Se_8$ are described.

Experimental

Synthesis. A stoichiometric combination of the pure elements, Ta powder(CERAC 99.9%), Ni powder(CERAC 99.9 %), and Se powder(Aldrich 99.99%) was mixed in a 2 : 1 : 7 mole ratio in a silica tube with the addition of a eutectic flux of CsCl/LiCl in a mass ratio of 5.5/1.0. The tube was then evacuated to $\sim 10^{-3}$ torr, sealed, and heated at 850 ℃ for 3 days. After this time the tube was cooled slowly over two days. Two kinds of single crystals were obtained. The major phase was found to be plate-like needles with shiny faces and it was proved to be the known ternary compound, Ta_2NiSe_7, by the X-ray diffraction analysis.[10] The minor phase was thick needle crystals and the presence of Ta, Ni, and Se was confirmed with the electron microprobe of an EDAX-equipped AMRAY scanning electron microscope.

Crystallographic Studies. A long needle-like crystal with approximate dimensions of 1.6 by 0.06 by 0.06 mm bounded by faces of the form {100}{010}{001} was selected for X-ray analysis. In spite of the risk caused by high absorption, we had no choice but to use such a large crystal for X-ray diffraction works. Preliminary examination and data collection were performed with Mo $K\alpha_1$ radiation ($\lambda=0.71073$ Å) on an MXC3 diffractometer (Mac Science) equipped with an incident beam monochromator graphite crystal. The unit cell parameters and the orientation matrix for data collection were obtained from the least-squares refinement, using the setting angles of 20 reflections in the range $20°<2\theta(\text{Mo K}\alpha)<28°$. The orthorhombic cell parameters and calculated volume are: $a=14.788(4)$ Å, $b=10.467(3)$ Å, $c=3.4563(8)$ Å, $V=535.0(2)$ Å^3. The systematic extinctions ($0kl: k=2n+1$, $h0l: h=2n+1$) were indicative of the space groups D_{2h}^9-*Pbam* or C_{2v}^8-*Pba*2. The centrosymmetric *Pbam* was assumed and subsequent refinements confirmed the choice of this space group.

Intensity data were collected with the ω-2θ scan technique. The intensities of two standard reflections, measured every hundred reflections, showed no significant deviations during the data collection. The scan rate was 5.0°/min (in ω axis), and the variable scan repetitions allowed one time data collection for intense reflections and assured good counting statistics for weak reflections where two or three times data collections were made. The data were corrected for absorption with the use of a linear absorption coefficient calculated for this composition.[11]

The initial positions for all atoms were obtained by using direct methods of the SHELXS-86 program.[12] The structure was refined by full matrix least squares techniques with the use of the SHELXL-93 program.[13] Anisotropic thermal motion and isotropic extinction parameters were included. The final cycle of refinement performed on F_o^2 with all 696 unique reflections afforded residuals wR2=0.1261 and conventional R index based on the reflections having $F_o^2>4\sigma(F_o^2)$ is 0.0448. A difference Fourier synthesis calculated with phase based on the final parameters showed no peak greater than 2.8% the height of a Ta atom. Additional crystallographic data and details from the data collection are given in Table 1. Positional parameters and equivalent isotropic thermal pa-

*To whom correspondence should be addressed.

Table 1. Details of X-ray Data Collection and Refinement

Formula mass, amu	1169.71
Space group	D_{2h}^9-*Pbam*
a, Å	14.788(4)
b, Å	10.467(3)
c, Å	3.4563(8)
V^a, Å^3	535.0(2)
Z	2
T, K	293(2)
Radiation	graphite monochromated MoKα_1 (λ(Kα_1)=0.71073 Å)
Linear absorption coefficient, cm^{-1}	527.08
Density (calc. g/cm^3)	7.261
Crystal size, mm^3	1.60×0.06×0.06
Scan type	ω-2θ
Scan speed, deg. min^{-1}	5.0 in ω
Scan range, deg.	1.0+0.35 tanθ
2θ limits, deg.	5°≤2θ(MoKα_1)≤55°
Data collected	$+h$, $+k$, $+l$
No. of unique data	691
No. of unique data with $F_o^2>4\sigma(F_o^2)$	661
wR2	0.1261
R (on F for $F_o^2>4(F_o^2)$)	0.0448
Goodness-of-fit on F^2	1.149

[a]α, β, and γ were constrained to be 90° in the refinement of cell constraints.

Table 2. Atomic Coordinates (×10^4) and Equivalent Isotropic Displacement Parameters (Å^2×10^3) for $Ta_2Ni_3Se_8$

Atom	Wyckoff notation	Site symmetry	*x*	*y*	*z*	U_{eq}
Ta(1)	4*g*	*m*	1188(1)	2055(1)	5000	7(1)
Ni(1)	2*a*	2/*m*	0	0	0	10(1)
Ni(2)	4*g*	*m*	2210(1)	3709(2)	0	8(1)
Se(1)	4*g*	*m*	−109(1)	2235(2)	0	9(1)
Se(2)	4*g*	*m*	1562(1)	282(1)	0	7(1)
Se(3)	4*g*	*m*	2870(1)	2464(2)	5000	9(1)
Se(4)	4*h*	*m*	1257(1)	4484(2)	5000	9(1)

Note. U_{eq} is defined as one third of the trace of the orthogonalized U_{ij} tensor.

rameters are given in Table 2. Table 3 lists anisotropic thermal parameters.

Electrical Conductivity Measurements. Four-probe dc conductivity measurements of the selected single crystals were made along the needle axis (*c*-axis), monitoring the temperature with a silicon diode sensor and Lake Shore DRC 91C controller together. Crystals of typical length of 1-3 mm and width of 0.01-0.02 mm were mounted on 0.020 mm gold wires using the commercially available silver paste, and put into the cryogenic system equipped with the conductivity measuring units described elsewhere.[14]

Table 3. Anisotropic Displacement Parameters (Å^2×10^3) for $Ta_2Ni_3Se_8$

Atom	U_{11}	U_{22}	U_{33}	U_{23}	U_{13}	U_{12}
Ta(1)	5(1)	7(1)	8(1)	0	0	0(1)
Ni(1)	3(1)	8(1)	18(2)	0	0	−1(1)
Ni(2)	6(1)	8(1)	9(1)	0	0	0(1)
Se(1)	6(1)	11(1)	10(1)	0	0	1(1)
Se(2)	5(1)	8(1)	9(1)	0	0	0(1)
Se(3)	6(1)	11(1)	10(1)	0	0	1(1)
Se(4)	9(1)	8(1)	11(1)	0	0	0(1)

Note. The anisotropic displacement exponent takes the form exp $[-2\pi^2(h^2a^{*2}U_{11}+\cdots+2hka^*b^*U_{12})]$.

Table 4. Selected Bond Lengths [Å] and Angles [deg] in $Ta_2Ni_3Se_8$

Ta-2Se(1)	2.589(1)		
Ta-2Se(2)	2.596(1)	Se(1)-Ta-Se(1)	83.77(6)
Ta-Se(3)	2.524(2)	Se(1)-Ta-Se(2)	76.45(4)
Ta-Se(4)	2.544(2)	Se(1)-Ta-Se(4)	87.55(5)
Ta-2Ni(1)	3.2711(7)	Se(3)-Ta-Se(4)	77.92(5)
Ta-2Ni(2)	2.875(2)		
Ta-2Ta	3.456(1)		
Ni(1)-2Se(2)	2.329(2)	Se(1)-Ni(1)-Se(2)	86.67(5)
Ni(1)-2Se(1)	2.345(2)		
Ni(1)-2Ni(1)	3.4563(8)		
Ni(2)-2Se(4)	2.372(2)	Se(2)-Ni(2)-Se(3)	93.66(8)
Ni(2)-2Se(3)	2.374(2)	Se(2)-Ni(2)-Se(3)	93.43(9)
Ni(2)-Se(2)	2.451(3)	Se(3)-Ni(2)-Se(4)	84.35(4)
Ni(2)-Ni(2)	3.4563(8)	Se(3)-Ni(2)-Se(4)	164.2(1)

Results and Discussion

The result of the single crystal study of $Ta_2Ni_3Se_8$ demonstrates the existence of another phase of the $Nb_2Pd_3Se_8$ family. Selected bond distances and angles for the compound $Ta_2Ni_3Se_8$ are given in Table 4. A drawing of the structure is given in Figure 1. This compound is isostructural with $Nb_2Pd_3Se_8$, $Ta_2Pt_3Se_8$, $Ta_2Ni_3S_8$, and $Ta_2Pd_3Se_8$, and the description of this structural type has been given in detail previously.[6,7] In general, the structural features in $Ta_2Ni_3Se_8$ follow the same trends as those in $Nb_2Pd_3Se_8$ family though they exhibit a little difference in bond lengths, bond angles, and unit cell parameters from the corresponding atoms.

As shown in Figure 2, the structure of $Ta_2Ni_3Se_8$ is composed of two chains of edge-sharing Se trigonal prisms centered by Ta atoms and bridged by Ni atoms bound to four coplanar Se atoms. Other Ni atoms capping into the chains are coordinated by edge-sharing Se square-pyramid. These chains are interconnected so as to form a structure with one-dimensional channels along the needle-axis (*c*-axis) as shown in Figure 1.

The Ni(1)-Se and Ni(2)-Se distances are not changed significantly even if geometries varied from square planar to

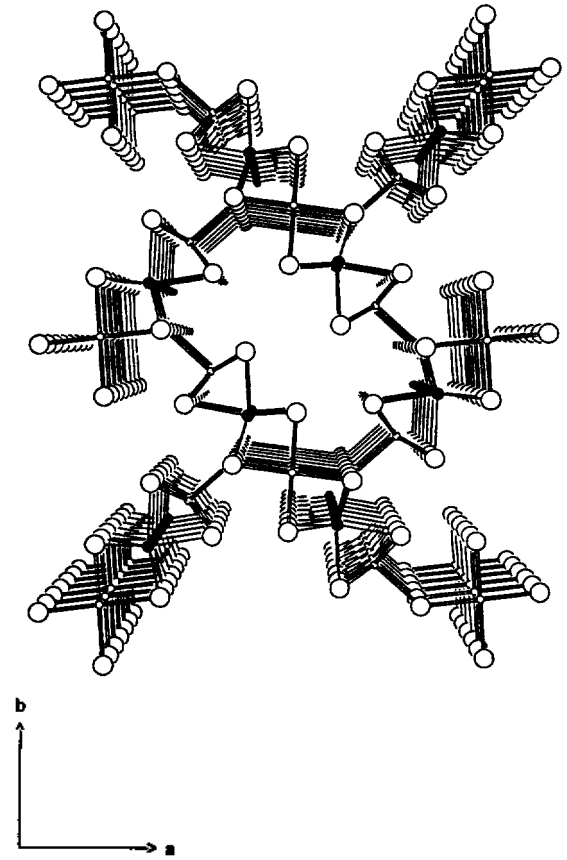

Figure 1. Perspective view along the c-axis. Ta atoms are small filled circles; Ni atoms are small open circles; Se atoms are large open circles.

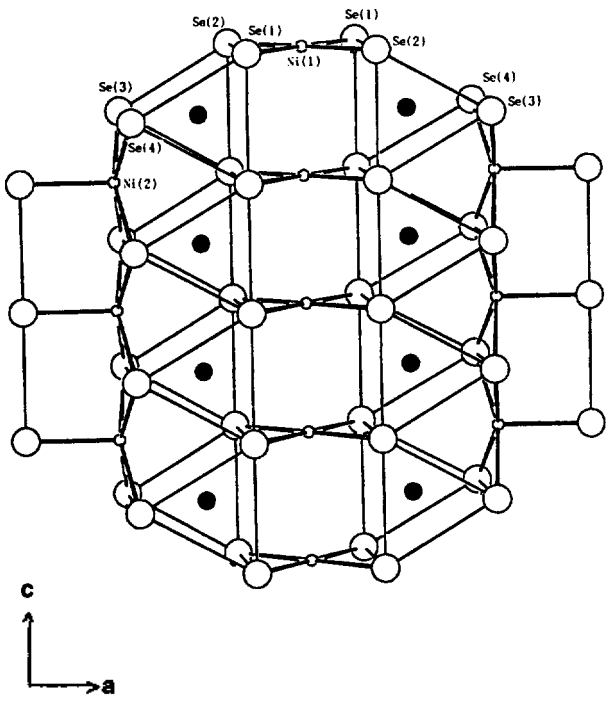

Figure 2. Individual chain in $Ta_2Ni_3Se_8$ along the b-axis. Ta atoms are small filled circles; Ni atoms are small open circles; Se atoms are large open circles.

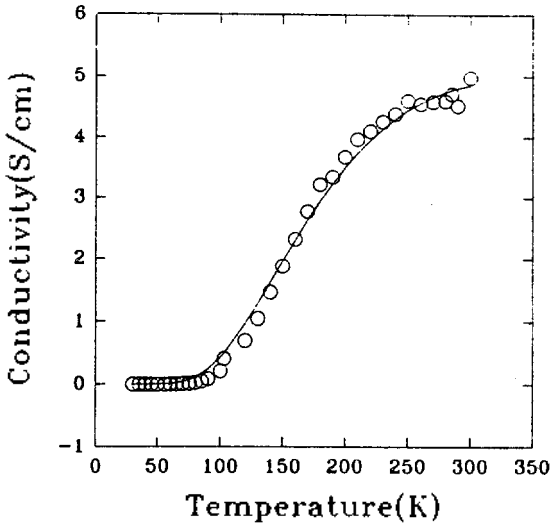

Figure 3. Temperature dependence of the single crystal conductivity along the needle axis c for $Ta_2Ni_3Se_8$ (o; observed, solid line; calculated).

square pyramid. The apical distance Ni(2)-Se(2), 2.451(3) Å of the square pyramid is somewhat longer than the basal distance, Ni(2)-Se(3), 2.374(2) Å, and Ni(2)-Se(4), 2.372(2) Å. The Ni(2) atom lying above the basal plane of the square pyramid has the resultant angle Se(3)-Ni(2)-Se(4) of 164.2(1)° which is in satisfactory agreement with the theoretical value, 164°, for the ideal C_{4v}-square pyramidal fragment ML_5 where M is a d^8 atom.[15]

The room temperature conductivity (~4.5 S/cm) is also similar to that of the isostructural compound, $Nb_2Pd_3Se_8$.[6,7] The temperature dependence of the single crystal conductivity in the temperature range of 300-30 K is plotted in Figure 3 together with the calculated values for the one-dimensional conductor according to the relation $\sigma(T)=AT^{-\alpha}\exp(-\Delta/T)$, which has been used for fitting the temperature dependence of the conductivity for such materials.[16] A least-squares fit of the data to the above relation affords $A=8.13\times10^5$ K$^{\alpha}$S/cm, $\alpha=2.10$, and $\Delta=707$ K for the $Ta_2Ni_3Se_8$. According to Epstein and Conwell,[6] the pre-exponential term may be related to the temperature dependent mobility and the exponential term to the activation of the carriers in a narrow band gap semiconductor. From this interpretation the compound, $Ta_2Ni_3Se_8$, should be classified as a semiconductor.[17] The d^0 (Nb^V) and d^8 (Pd^{II}) atoms are responsible for the semiconducting behavior. The crystallographic and electrical conductivity data indicate that the classical valence description for the compound should be $(Ta^{5+})_2(Ni^{2+})_3(Se^{2-})_8$.

Acknowledgments. This research was supported by the Korean Science and Engineering Foundation (KOSEF).

References

1. (a) Matthias, B. T.; Marezio, M.; Corenzwit, E.; Cooper, A. S.; Barz, H. E. *Science.* **1972**, *175*, 1465. (b) Mato, Y.; Yoyota, N.; Noto, K.; Hoshi, A. *Phys. Lett. A* **1973**, *45*, 99. (c) Ravaine, D. J. *Non-Cryst. Solids.* **1985**, *73*, 287.
2. (a) Whittingham, M. S. *Prog. Solid State Chem.* **1978**, *12*, 41. (b) Rouxel, J.; Brec, R. *Annu. Rev. Mater. Sci.* **1986**,

16, 137.
3. (a) Di Salvo, F. J. *Surf. Sci.* **1976**, *58*, 297. (b) Monceau, P., Ed.; D. Reidel: Dordrecht, *Electronic Properties of Inorganic Quasi-One-Dimensional Compounds*; 1985; Parts 1, 2.
4. Wells, A. F. *Structural Inorganic Chemistry*; 5th Ed.; Oxford University Press: New York, U.S.A., 1984; p 11 00.
5. Rao, C. N. R.; Gopalakrishnan, Frsj. *New directions in solid state chemistry*; Cahn, R. W., Ed.; Cambridge University Press: Cambridge, 1986; Chap. 6.
6. Keszler, D. A.; Ibers, J. A. *J. Solid State Chem.* **1984**, *52*, 73.
7. Sunshine, S. A.; Keszler, D. A.; Ibers, J. A. *Acc. Chem. Res.* **1987**, *20*, 395.
8. Keszler, D. A.; Ibers, J. A.; Shang, M.; Lu, J. *J. Solid State Chem.* **1985**, *57*, 68.
9. Squattrito, P. J.; Sunshine, S. A.; Ibers, J. A. *J. Solid State Chem.* **1986**, *64*, 261.
10. Sunshine, S. A.; Ibers, J. A. *Inorg. Chem.* **1985**, *25*, 43 55.
11. The analytical method as employed in the Northwestern absorption program, AGNOST, was used for the absorption correction (de Meulenaer, J.; Tompa, H. *Acta Crystallogr.* **1965**, *19*, 1014.).
12. Sheldrick, G. M. *Acta Cryst.* **1990**, *A46*, 467.
13. Sheldrick, G. M. *SHELXL 93, Program for the Refinement of Crystal Structures*; University of Göttingen, 1993.
14. Lee, Young-Ju; Jung, Chan-Sun; Sin, Hee-Kyoon. *J. Kor. Phys. Soc.* **1993**, *26*, 503.
15. Rossi, A. R.; Hoffmann, R. *Inorg. Chem.* **1975**, *14*, 365.
16. Epstein, A. J.; Conwell, E. M.; Sandman, D. J.; Miller, J. S. *Solid State Commun.* **1977**, *23*, 355.
17. Epstein, A. J. *Molecular Metals*; Hatfield, W. E., Ed.; Plenum Press: New York, U.S.A., 1979; p 155.

A Theory on Phase Behaviors of Diblock Copolymer/Homopolymer Blends

Kyung-Sup Yoon and Hyungsuk Pak*

Department of Chemistry, Seoul National University, Seoul 151-742, Korea
Received July 6, 1995

The local structural and thermodynamical properties of blends A-B/H of a diblock copolymer A-B and a homopolymer H are studied using the polymer reference interaction site model (RISM) integral equation theory with the mean-spherical approximation closure. The random phase approximation (RPA)-like static scattering function is derived and the interaction parameter is obtained to investigate the phase transition behaviors in A-B/H blends effectively. The dependences of the microscopic interaction parameter and the macrophase-microphase separation on temperature, molecular weight, block composition and segment size ratio of the diblock copolymer, density, and concentration of the added homopolymer, are investigated numerically within the framework of Gaussian chain statistics. The numerical calculations of site-site interchain pair correlation functions are performed to see the local structures for the model blends. The calculated phase diagrams for A-B/H blends from the polymer RISM theory are compared with results by the RPA model and transmission electron microscopy (TEM). Our extended formal version shows the different feature from RPA in the microscopic phase separation behavior, but shows the consistency with TEM qualitatively. Scaling relationships of scattering peak, interaction parameter, and temperature at the microphase separation are obtained for the molecular weight of diblock copolymer. They are compared with the recent data by small-angle neutron scattering measurements.

Introduction

The *interaction parameter* (χ parameter or interaction energy)[1-6] is considered as a gauge of interaction between the polymer chains and as a *black box* in the field of polymer science. χ parameter associated with the enthalpy of mixing is an important characteristic one in high molecular weight polymer systems. A great flux of activities thus has been pursued *to understand the fundamental concept of* χ *parameter.* Such χ parameter also can be used to predict phase separations because it governs phase behaviors of polymer blends. The phase separation behaviors are common in polymeric materials, particularly when two different polymers are present as the form of blends and/or block copolymers.

Many theoretical and experimental studies have been used in conjunction with scattering data[7-19] and Monte Carlo (MC) simulations[20,21] to provide important tools in studies of thermodynamic interactions in polymer mixtures. Among these theoretical studies the most typical two models are the well known Flory-Huggins lattice model (FHLM)[1] and the random phase approximation (RPA) model[2] developed initially by de Gennes. Flory-Huggins χ parameter is only treated as a function of temperature, $\chi \propto 1/T$. Many experimental results show that χ parameter is affected by molecular weight and